Geodesic Active Contours with Combined Shape and Appearance Priors

Rami Ben-Ari[1] and Dror Aiger[1,2]

[1] Orbotech LTD, Yavneh, Israel
[2] Ben Gurion University, Be'er Sheva, Israel
{rami-ba,dror-ai}@orbotech.com

Abstract. We present a new object segmentation method that is based on *geodesic active contours* with combined shape and *appearance* priors. It is known that using shape priors can significantly improve object segmentation in cluttered scenes and occlusions. Within this context, we add a new prior, based on the appearance of the object, (i.e., an image) to be segmented. This method enables the appearance pattern to be incorporated within the geodesic active contour framework with shape priors, seeking for the object whose boundaries lie on high image gradients and that best fits the shape and appearance of a reference model. The output contour results from minimizing an energy functional built of these three main terms. We show that appearance is a powerful term that distinguishes between objects with similar shapes and capable of successfully segment an object in a very cluttered environment where standard active contours (even those with shape priors) tend to fail.

1 Introduction

Segmentation is a fundamental topic in image processing. Variational methods solve this problem by means of energy minimization. Methods belonging to this class are generally divided into two types, the *region*-based and the *edge*-based methods. The region based approaches [1, 2] often make use of the minimal variance criterion, i.e., seeking for a curve that would best separate the interior and exterior of the object with respect to their relative average intensities. The drawback of these methods appear when the contrast of a desired object or part of it, is low with respect to the background. The segmentation outcome then labels partially or the whole object as background.

On the other hand, the edge-based active contour methods separate an object from its surroundings by locating the object boundaries in the image. They use a dynamically evolving curve to minimize an energy functional, that presents a non-Euclidean length of the segmenting contour. The minimum occurs when the curve coincides with points of high gradient in the image. Assuming that object edges are characterized by relatively high intensity variations, the active contour then becomes stationary when it reaches the object's boundary. Historically, the active contours were pioneered with the classical snakes [3, 4], followed by non-variational geometric active contours [5] and the geodesic active contours

J. Blanc-Talon et al. (Eds.): ACIVS 2008, LNCS 5259, pp. 494–505, 2008.

(GAC) [6, 7, 8]. The GAC presents a robust geometric alternative for the two previous types of active contour methods.

The level-set based contour representations [9] have become a popular framework for image segmentation [1, 8, 7]. They permit topological changes in the evolving contour and are also used to exploit various low level image properties such as edge information [6, 7, 8] and intensity homogeneity [1, 2].

In recent years, much effort has been made to integrate prior knowledge into level-set based segmentation. This was done to make the segmentation process more robust to misleading low-level information caused by noise, background clutter, low contrast and partial occlusion [10,11,12,13]. The most common prior is obtained by representation of a reference *shape* within the energy functional. The recovered object boundary is then required to resemble an expected type of contour, in addition to being constrained by the segmentation criterion (e.g., minimum variance or GAC). Several studies cover segmentation with shape prior [10,11,12,13], almost all of them are a linear combination of a basic segmentation criterion and a shape dissimilarity measure. These works mainly differ in the determination of a suitable shape representation and the corresponding similarity measure with a reference shape. While similarity transformations are frequently employed [12, 10, 11], Raviv et al., [13] recently published a method allowing for a more general projective transformation of the object's shape.

In fact, an image may contain a group of objects with similar shapes or shapes that can be transformed to each other by the allowed transformation (e.g., scale or rotation). In such case the shape prior encounters an ambiguity and therefore is not capable of discriminating between the objects of the group. Moreover, scenes with high level of clutter can have many local minimas where the evolved contour may be trapped. In these cases there is a need for higher prior support in the segmentation process than just a shape model.

In this work, we consider prior knowledge provided by a similar template, i.e., prior shape and appearance of an object. Finding an object in the image that matches a given view is well known as template matching. There are several methods for handling this problem, e.g., Normalized Cross Correlation or more advanced methods such as that discussed by Hel-Or and Hel-Or [14]. Frequently these methods perform a *rigid* matching, where the object boundaries are fitted to an isometry transformation of the template. In this respect Freedman and Zhang [15] suggested a method with *elastic* matching, i.e. allowing for non-linear deformation of a model (or pattern), based on histogram similarity to a prior appearance pattern.

The ability of GAC in elastic shape matching was already shown by Chen et al. [11]. In this paper we suggest a new geodesic active contour model that incorporates a coupled shape and appearance priors, which are both allowed to transform under an extended similarity transformation (i.e., with different scales in the spatial directions). Our novel appearance similarity measure is based on intensity differences. The input to the suggested method includes an image for segmentation and a reference model to be used as a prior. The model may describe a deformed view of the desired object.

The final segmentation is an outcome of an energy based curve evolution, where the minimum cost function also satisfies a new appearance similarity. In the emerged method the evolving template is attracted toward the desired object allowing the elastic segmentation contour to bypass the misleading objects and local minimas of a standard GAC method.

2 Formulation

Consider a normalized gray level image $I : \Omega \to [0, 1]$, where Ω is the image domain. Let $C : [0, L] \to \mathbb{R}^2$ denote a planar curve given in a parametric representation which consists of the boundaries of the objects in the image. The geodesic active contour (GAC) method for segmentation is known as minimization of the following functional [6]:

$$E_{GAC}(C) = \int_0^L g(C(s))ds. \tag{1}$$

This functional is an integration of an inverse edge detector function along the contour. We choose g as:

$$g(|\nabla I|) = \frac{1}{1 + K|\nabla(G_\sigma * I)|^2}. \tag{2}$$

where K represents a magnification factor, G_σ represents a Gaussian with standard deviation σ and $*$ denotes the standard convolution operator. Note that $g(|\nabla I|) \to 1^-$ in homogeneous regions and $g(|\nabla I|) \to 0^+$ on edges. Minimization of the functional (1) defines a search for a curve which results in the smallest possible values of $g(C(s))$ in the image domain. The so-called edge detector g determines a *metric* [16] for the curve length in $\mathbb{R}^2$ [6]. A well-known example in this case is $g(x, y) = 1$, for which the functional measures the Euclidean length of the curve.

In the level set formulation for curve evolution [9] the segmenting boundary C is the zero level set of a 3D function ϕ, for which $C = \{\mathbf{x} \in \Omega | \phi(\mathbf{x}) = 0\}$. The GAC functional in terms of level-set formulation is then [7]:

$$E_{GAC}(\phi) = \int_\Omega g(|\nabla I|)|\nabla H(\phi)|d\mathbf{x}, \tag{3}$$

where $H(\phi)$ is the *Heaviside* function of the evolving ϕ,

$$H(\phi) = \begin{cases} 1 & \phi > 0 \\ 0 & \phi \leq 0 \end{cases} \tag{4}$$

and $|\nabla H(\phi)|$ indicates the length of the zero level-set curve [17].

When a good estimation of the edge orientation is provided, an *alignment* term is often added to the energy functional [18]. This term requires co-linearity

between the image gradient and the contour normal. Formally this requirement is presented by the term,

$$E_{Al}(\phi) = -\int_{\Omega} |\langle \nabla I, \frac{\nabla \phi}{|\nabla \phi|} \rangle| |\nabla H(\phi)| d\mathbf{x}. \tag{5}$$

in the energy functional [7].

Our preliminary energy functional without any semantic priors is a linear combination of the two mentioned terms:

$$E_{GA}(\phi) = E_{GAC} + \gamma_{al} E_{Al}, \tag{6}$$

where γ_{al} is a positive weight factor. This functional is similar to the one derived in [8, 7].

2.1 Shape Prior

The energy functional in (6) can be extended by adding a shape prior [10, 11, 12, 19, 13]. Rousson and Paragios [20] represented the shape surrounding a region Ω_s by the corresponding sign distance function related to the boundary, introducing a unique level set function:

$$\phi_s = \begin{cases} < 0 \; x \in \Omega_s \backslash \partial\Omega_s \\ = 0 \; x \in \partial\Omega_s \\ > 0 \text{ otherwise} \end{cases} \tag{7}$$

$$|\nabla \phi_s| = 1.$$

Cremers et al. [20] adopted the shape representation in (7) to define a measure for shape dissimilarity:

$$E_S = \int_{\Omega} (\phi - \phi_s)^2 d\mathbf{x}, \tag{8}$$

This model does not allow for any transformation of the shape (e.g., translation, rotation or scaling). Consequently, the global minimum of the energy functional in (8) is obtained when the prior shape is placed exactly at the location of the desired object, having the same pose and scale as the object. These requirements present a frail constraint for the segmentation process, demanding for an exact shape model as a prior. Such condition is rarely satisfied in real applications.

In order to remove the constraint for use of distance functions and allow for deformation of the prior shape, we consider the following L^2 shape dissimilarity measure [10, 13]:

$$E_S = \int_{\Omega} \left(H(\phi) - H(\tilde{\phi}_s) \right)^2 d\mathbf{x} \tag{9}$$

where

$$\tilde{\phi}_s(\mathbf{x}) := \phi_s \left(P \left[T^{-1}(\mathbf{x}_h) \right] \right)$$

and $T(\cdot)$ denotes a certain type of transformation (such as, similarity or affine) of the shape prior that should be revealed in the solution. Note that T acts

on the homogeneous coordinates, i.e., $\mathbf{x}_h := (x, y, 1)^T$, and the operator P is a projection:

$$P(x, y, 1) = (x, y). \tag{10}$$

In the dissimilarity measure (9) the evolving level set ϕ and the shape level set function $\tilde{\phi}_s$ are not forced any more to resemble each other, nor are they constrained to be distance functions. Instead, we demand the similarity of the regions within the corresponding zero set contours. As for the transformation T, several transformations may be considered, ranging from identity transformation [12] to similarity (isometry) [10, 11] and projective transformations [13]. In this work we choose an extended similarity transformation i.e., a similarity, where different scales in each direction are allowed. This choice presents a trade-off between simplicity and accuracy, although one can also incorporate a more general transformation into our framework. Consequently, the relation between the reference model and the one currently used in the evolution scheme is defined by the following variables: translation $(\mathsf{t_x}, \mathsf{t_y})^T$, planar rotation θ and two scale factors $\mathsf{s_x}, \mathsf{s_y}$. We also consider the rotation and scales relative to the center of the area of the evolving prior shape $(x_g, y_g)^T$. The inverse map for our transformation then emerges as:

$$\begin{pmatrix} \tilde{x} \\ \tilde{y} \end{pmatrix} := P\left[T^{-1}(\mathbf{x}_h)\right] = \begin{pmatrix} \frac{1}{\mathsf{s_x}}\left[(x - x_g - \mathsf{t_x})\cos\theta + (y - y_g - \mathsf{t_y})\sin\theta + x_g\right] \\ \\ \frac{-1}{\mathsf{s_y}}\left[(x - x_g - \mathsf{t_x})\sin\theta + (y - y_g - \mathsf{t_y})\cos\theta + y_g\right] \end{pmatrix}. \tag{11}$$

2.2 Appearance Prior

The prior soft constraint can be extended by adding an image to the prior shape, i.e., an appearance model. Although we perform this novel extension for a GAC application [11, 19], the suggested appearance term can equally be added to a region-based method [10, 13, 12].

Given an image on the prior shape domain ,$I_p : \Omega_s \to [0, 1]$ we define the embedded prior image, $I_p^e : \Omega \to [0, 1]$ as:

$$I_p^e = \begin{cases} I_p & \mathbf{x} \in \Omega_s \\ c \in [0, 1] & \mathbf{x} \in \Omega \backslash \Omega_s \end{cases} \tag{12}$$

Since the shape prior presents the boundary of I_p we evolve the shape and the image by the same transformation $T(\cdot)$:

$$\tilde{I}_p^e = I_p^e\left(P\left[T^{-1}(\mathbf{x}_h)\right]\right). \tag{13}$$

Defining the appearance dissimilarity as a L^2 measure for intensity discrepancy over the shape's domain, we suggest the following term for the appearance prior:

$$E_{Ap} = \int_\Omega \left(\tilde{I}_p^e - I\right)^2 \left(1 - H(\tilde{\phi}_s)\right) d\mathbf{x}. \tag{14}$$

One can easily realize that the appearance dissimilarity measure vanishes when the prior image coincides with its matching part in the image.

2.3 The Energy Functional

By adding the prior shape and appearance terms (9, 14) to our preliminary GAC model (6), we obtain the following energy functional:

$$E(\phi, T) = E_{GAC} + \gamma_{al} E_{Al} + \frac{\gamma_s}{2} E_S + \frac{\gamma_{ap}}{2} E_{Ap}, \tag{15}$$

or explicitly,

$$\begin{aligned} E(\phi, T) = \int_\Omega & g(|\nabla I|)|\nabla H(\phi)| - \gamma_{al} |\langle \nabla I, \frac{\nabla \phi}{|\nabla \phi|} \rangle| |\nabla H(\phi)| \\ & + \frac{\gamma_s}{2} \left(H(\phi) - H(\tilde{\phi}_s) \right)^2 + \frac{\gamma_{ap}}{2} \left(\tilde{I}_p^e - I \right)^2 \left(1 - H(\tilde{\phi}_s) \right) d\mathbf{x}. \end{aligned} \tag{16}$$

Formally we search for a level set function ϕ and a transformation of the reference model (shape and appearance) that minimizes the functional (16). The solution is then a ϕ with zero level set that best satisfies the GAC requirement (i.e., a contour lying on high image gradients) while fitting the transformed version of the reference model (given by $\tilde{I}_p^e, \tilde{\phi}_s$). The additional appearance (soft) constraint is satisfied when the evolved shape prior coincides with the object similar to the reference model.

This concludes the description of our model. In the next section we present the numerical scheme for minimization of the above energy functional.

3 Minimization

The segmentation process is generated by minimizing the functional in (16). To this end, we employ the common gradient descent evolution equations derived from the Euler-Lagrange PDEs. We alternately update the level set function ϕ and the transformation parameters till convergence.

3.1 The Segmentation Level-Set Function

For a fixed shape and appearance model, the level set function ϕ evolves according to the gradient descent method by:

$$\frac{\partial \phi}{\partial t} = \left[\text{div} \left(g\left(|\nabla I|\right) \frac{\nabla \phi}{|\nabla \phi|} \right) - \gamma_{al} \text{sign} \langle \nabla \phi, \nabla I \rangle \triangle I + \gamma_s \left(H(\phi) - H(\tilde{\phi}_s) \right) \right] \delta(\phi), \tag{17}$$

where $\triangle$ stands for *Laplacian* and $\delta(\cdot)$ is the *Dirac* function. Note that the curve evolution is influenced by the appearance through the shape prior. On one hand minimization of the the appearance dissimilarity measure, creates a transformation that drives the reference model towards the object. On the other hand the segmentation contour is attracted to the reference's shape in order to minimize

the shape dissimilarity. The evolution ultimately drives the segmentation contour toward an object with similar shape and appearance to our reference model. This procedure is also efficient in overcoming the notorious problem of GAC local minimas.

Practically, a smooth approximation of the Heaviside and Dirac functions are used [1]:

$$H_\epsilon(\phi) = \frac{1}{2}\left(1 + \frac{2}{\pi}\arctan\left(\frac{\phi}{\epsilon}\right)\right), \tag{18}$$
$$\delta_\epsilon(\phi) = \frac{dH_\epsilon(\phi)}{d\phi} = \frac{1}{\pi}\frac{\epsilon}{\epsilon^2 + \phi^2}$$

The minimization of (17) is carried out subjected to the Neumann boundary condition. All spatial derivatives are approximated by central differences. Still the divergence term in (17) is handled differently since the division by $|\nabla\phi|$ often imposes a numerical instability. To this end, we employ a semi-implicit scheme for discretization of this term as performed in [2].

3.2 Recovery of Transformation

Minimization of the energy functional (16) by a gradient descent scheme involves evolution of the level-set function ϕ simultaneously with the recovery of the transformation T. The transformation parameters $(\mathsf{t_x}, \mathsf{t_y}, \mathsf{s_x}, \mathsf{s_y}, \theta)$ are gained by solving the associated Euler-lagrange equations. To this end, we again use the gradient descent approach:

$$\begin{aligned}
\frac{\partial \mathsf{t_x}}{\partial t} &= \int_\Omega (f_s + f_{a_1})\left(\frac{\phi_{sx}}{\mathsf{s_x}}\cos\theta - \frac{\phi_{sy}}{\mathsf{s_y}}\sin\theta\right) \\
&\qquad + f_{a_2}\left(\frac{I_{sx}}{\mathsf{s_x}}\cos\theta - \frac{I_{sy}}{\mathsf{s_y}}\sin\theta\right) d\mathbf{x} \\
\frac{\partial \mathsf{t_y}}{\partial t} &= \int_\Omega (f_s + f_{a_1})\left(\frac{\phi_{sx}}{\mathsf{s_x}}\sin\theta + \frac{\phi_{sy}}{\mathsf{s_y}}\cos\theta\right) \\
&\qquad + f_{a_2}\left(\frac{I_{sx}}{\mathsf{s_x}}\sin\theta + \frac{I_{sy}}{\mathsf{s_y}}\cos\theta\right) d\mathbf{x} \\
\frac{\partial \mathsf{s_x}}{\partial t} &= \int_\Omega (f_s + f_{a_1})\frac{\phi_{sx}}{\mathsf{s_x}}(\tilde{x} - x_g) + f_{a_2}\frac{I_{sx}}{\mathsf{s_x}}(\tilde{x} - x_g)\, d\mathbf{x} \\
\frac{\partial \mathsf{s_y}}{\partial t} &= \int_\Omega (f_s + f_{a_1})\frac{\phi_{sy}}{\mathsf{s_y}}(\tilde{y} - y_g) + f_{a_2}\frac{I_{sy}}{\mathsf{s_y}}(\tilde{y} - y_g)\, d\mathbf{x} \\
\frac{\partial \theta}{\partial t} &= \int_\Omega (f_s + f_{a_1})\left(\phi_{sy}\frac{\mathsf{s_x}}{\mathsf{s_y}}(\tilde{x} - x_g) - \phi_{sx}\frac{\mathsf{s_y}}{\mathsf{s_x}}(\tilde{y} - y_g)\right) \\
&\qquad + f_{a_2}\left(I_{sy}\frac{\mathsf{s_x}}{\mathsf{s_y}}(\tilde{x} - x_g) - I_{sx}\frac{\mathsf{s_y}}{\mathsf{s_x}}(\tilde{y} - y_g)\right)
\end{aligned} \tag{19}$$

where $\tilde{x}, \tilde{y}$ are given in (11), the subscripts x, y indicate partial derivatives and,

$$\begin{aligned} f_s &:= \gamma_s \left(H(\phi_s) - H(\phi)\right) \delta(\phi_s) \\ f_{a_1} &:= -\frac{\gamma_{ap}}{2} \left(\tilde{I}_s - I\right)^2 \delta(\phi_s) \\ f_{a_2} &:= \gamma_{ap} \left(\tilde{I}_s - I\right) \left(1 - H(\phi_s)\right). \end{aligned} \tag{20}$$

3.3 The Algorithm

We consider the following setup. The input consists of two images: I, describing the image including an object of interest, and I_s, the prior image with its boundary indicating the prior shape. Having an approximate appearance of the object at hand, one can use a template matching scheme (e.g., Normalized Cross Correlation) to initialize the prior shape location as close as possible to the desired object. Note that I_s is allowed to be a distorted object image in a noisy or cluttered background. Therefore an exact match from the NCC is not expected. The concurrent evolution of the transformation $T(\cdot)$ with the level set function ϕ allows us to gradually recover the view of the object in the correct pose, location and scale, obtained from the reference model. Our numerical scheme performs the following steps:

1. Given an arbitrary initial contour and a reference image of the object, construct the initial level-set functions ϕ and ϕ_s by signed distance functions. Although our level set functions are initialized by distance functions, the overhead of re-distance procedure is bypassed due to the special discretization of the divergence term [2].
2. Initialize (e.g., by identity map) the transformation parameters $\mathsf{t_x}, \mathsf{t_y}, \mathsf{s_x}, \mathsf{s_y}, \theta$.
3. Update ϕ using the gradient descent equation (17).
4. Update the transformation parameters $\mathsf{t_x}, \mathsf{t_y}, \mathsf{s_x}, \mathsf{s_y}, \theta$ using the evolution equations in (19).
5. Repeat steps 3 and 4 until convergence.

4 Experimental Results

The control parameters in our model correspond to the relative weights between the active contour, K, γ_{al}, the shape prior, γ_s and the appearance prior γ_{ap} criteria. One can adjust the parameters according to the class of problems in hand. Here, we first set the following parameters fixed, $\epsilon = 0.001, \gamma_{al} = 3$ and tune the other three according to the contrast, clutter and other visual cues.

In our first test we demonstrate the significance of the prior appearance model in a case where the shape prior encounters an ambiguity. Fig. 1(a) shows two views of a coin, each from a different side, presenting two objects with the same shape. The lower coin's image was darkened manually, to have a different appearance. In order to challenge our method, we first chose the darker coin with the lower contrast to be the desired object. To demonstrate the elastic matching ability, associated with

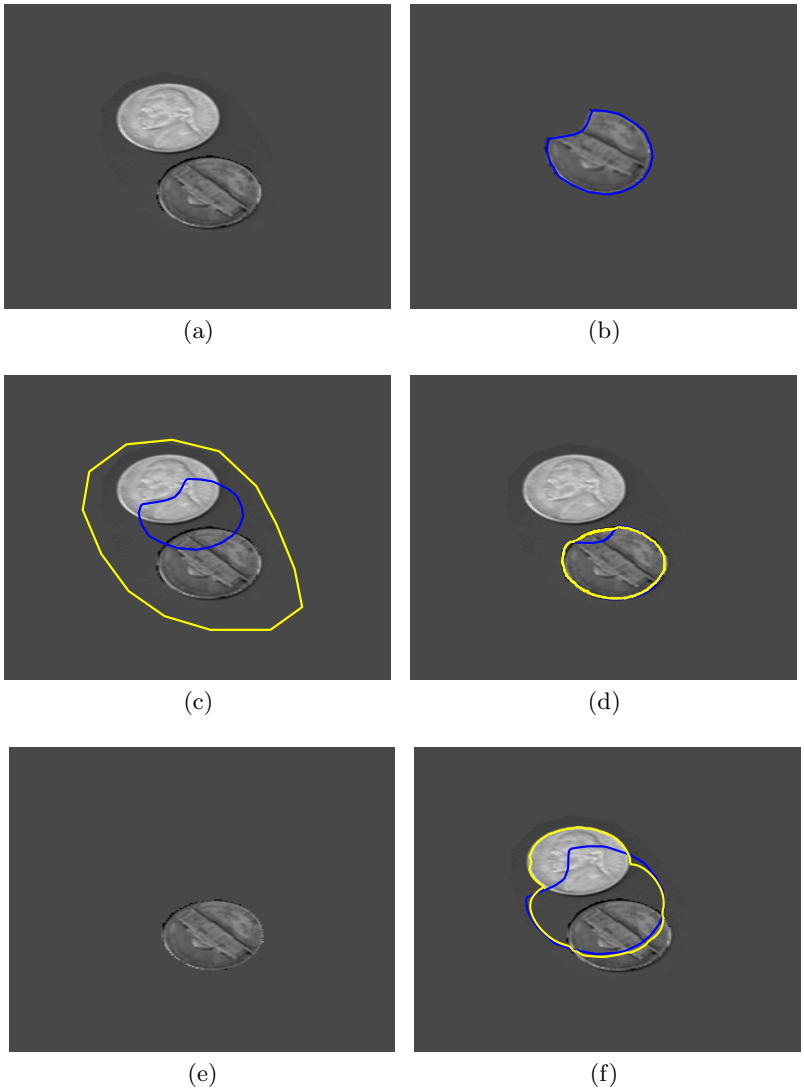

Fig. 1. An image of two objects having the same shape. (a) Input image. (b) The model (the shape model is the boundary, indicated by blue). (c) Initial contour (yellow) and prior shape (blue) (d) Output contour (yellow) and the boundary of the transformed reference model (blue). Parameter setting: $K = 800, \gamma_s = 0.75, \gamma_{ap} = 40$. (e) The image extracted from the interior of the output contour. (f) Segmentation result without the appearance prior (i.e., GAC+shape prior).

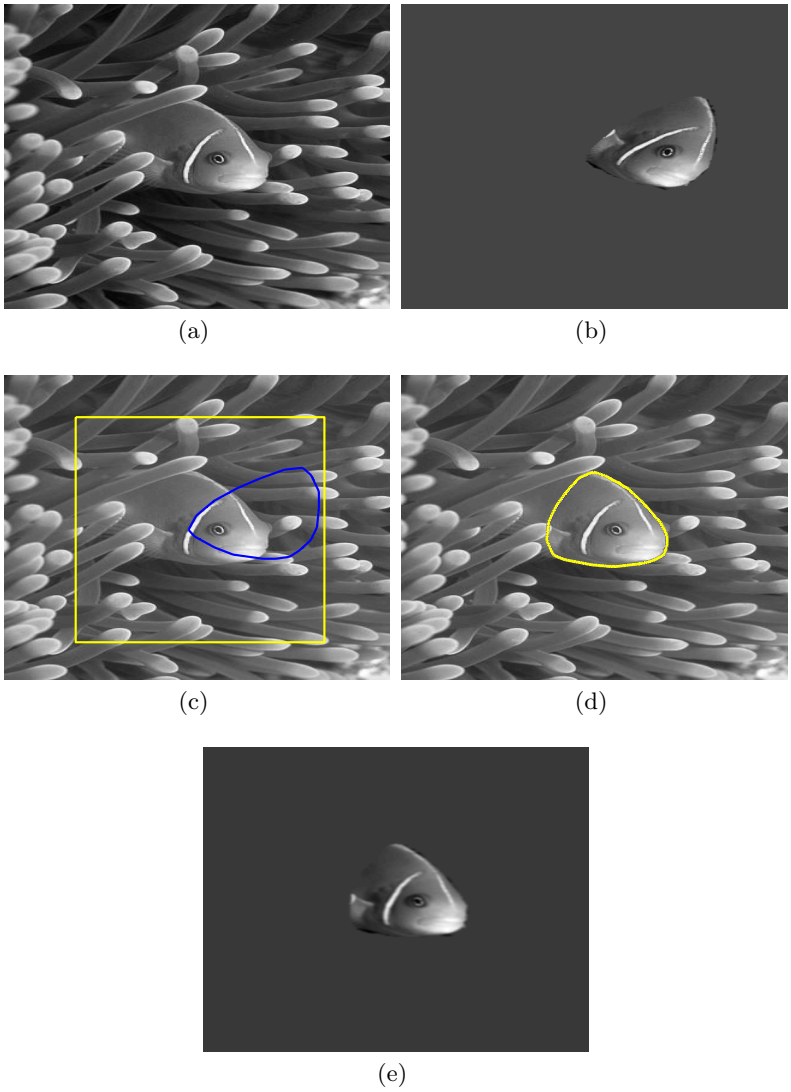

Fig. 2. High cluttered image with similarity warp of the model. (a) Input image. (b) The model (the shape model is the boundary). (c) Initial contour (yellow) and prior shape (blue). (d) Output contour (yellow). In this case the boundary of the transformed reference model coincides with the output contour. This successful result is achieved due to our appearance prior, presenting the most significant fidelity cue in the segmentation process. (e) The transformed reference model (shape and appearance). Parameter setting: $K = 100, \gamma_s = 5, \gamma_{ap} = 100$.

our variational model, the reference model was damaged by having a missing part and then distorted by a scale factor of $\mathsf{s}_\mathsf{x} = 1.2, \mathsf{s}_\mathsf{y} = 1$, and rotation $\theta = 15°$ (see Fig. 1(b). Moreover, the initial location of the reference model (the blue line in Fig. 1(c) was set to have a higher overlap with the wrong object.

The segmentation contour (the yellow curve) along with the recovered shape (blue) are shown in Fig. 1(d). The active contour was driven toward the desired object by the appearance prior, thus yielding a successful segmentation. For comparison, the result from our model without the appearance term (i.e., a model with GAC and shape prior) is shown in Fig. 1(f). In this case the reference model expands in order to align with the evolving contour, yielding an incorrect segmentation. The results also verify that our model can segment the object filling the gap in the reference shape. Note that the linearly transformed reference model cannot reach a successful match, since the correct transformation is non-linear.

In the second test (Fig. 2) we show the effectiveness of the appearance prior in a cluttered image. The reference model here is a shifted and a rotated version of the true object's image (by $\mathsf{t}_\mathsf{x} = 20, \mathsf{t}_\mathsf{y} = -20$ pixels and $\theta = 30°$). The results show that our model, with the additional appearance term, can overcome the high clutter in the image and extract the object successfully.

5 Summary and Future Work

This paper introduces a novel appearance prior in the context of variational segmentation methods. We suggest a GAC model, combining the shape and appearance priors. Our scheme makes use of a reference model, indicating an optionally distorted image and shape of the desired object in the scene. The energy minimization results a closed segmenting contour that presents a compromise between lying on high gradients and surrounding a patch of image that best matches a transformed version of the reference model. We allow the reference model to evolve by an extended similarity transformation. Although the segmentation target is linearly transformed (linear in the projective space) in the evolution process, the final segmentation contour presents a non-linear map of the reference model, due to the main GAC term. The performed tests demonstrate the capability of our method to handle a wide range of applications. These include segmentation of a required object in scenarios including objects with similar shapes but having different appearances (where common shape prior are tend to fail) and object segmentation in cluttered images.

A limitation to our model may arise when the reference model is distorted by large non-linear deformations, where the efficiency of the priors degrades. In our future work we intend to deal with this problem.

References

1. Chan, T., Vese, L.: Active contours without edges. IEEE Transactions on Image Processing 10, 266–277 (2001)
2. Vese, L.A., Chan, T.F.: A multiphase level set framework for image segmentation using the mumford and shah model. IJCV 50, 271–293 (2002)

3. Kass, M., Witkin, A., Terzopoulus: Snakes: Active contour models. IJCV 1, 321–331 (1998)
4. Terzopoulus, D., Witkin, A., Kass, M.: Constraints on deformable models: Recovering rigid shapes and nonrigid motions. Artificial Intelligence 36, 91–123 (1998)
5. Malladi, R., Sethian, J.A., Vemuri, B.: Shape modeling with front propogation: A level set approach. IEEE Trans. on PAMI 17, 158–175 (1995)
6. Caselles, V., Kimmel, R., Sapiro, G.: Geodesic active contours. IJCV 22, 61–79 (1997)
7. Kimmel, R.: Fast edge integration. In: Osher, S., Paragios, N. (eds.) Geometric Level Set Methods in Imaging Vision and Graphics. Springer, Heidelberg (2003)
8. Goldenberg, R., Kimmel, R., Rivlin, E., Rudzsky, M.: Fast geodesic active contours. IEEE Trans. on PAMI 10, 1467–1475 (2001)
9. Osher, S., Sethian, J.A.: Fronts propagating with curvature-dependent speed: Algorithms based on Hamilton-Jacobi formulations. Journal of Computational Physics 79, 577–684 (1988)
10. Chan, T., Zhu, W.: Level set based shape prior segmentation. In: CVPR, vol. 2, pp. 1164–1170 (2005)
11. Chen, Y., Tagare, H.D., Thiruvenkadam, S., Huang, F., Wilson, D., Gopinah, K., Briggs, R.W., Geise, E.A.: Using prior shapes in geometric active contours in a variational framework. IJCV 50, 315–328 (2002)
12. Cremers, D., Sochen, N., Schnörr, C.: Towards recognition-based variational segmentation using shape priors and dynamic labeling. In: Griffin, L.D., Lillholm, M. (eds.) Scale-Space 2003. LNCS, vol. 2695, pp. 388–400. Springer, Heidelberg (2003)
13. Riklin-Raviv, T., Kiryati, N., Sochen, N.: Prior-based segmentation and shape registration in the presence of projective distortion. IJCV 72, 309–328 (2007)
14. Hel-Or, Y., Hel-Or, H.: Real time pattern matching using projection kernels. IEEE Trans. on PAMI 27, 1430–1445 (2005)
15. Freedman, D., Zhang, T.: Active contours for tracking distributions. IEEE Trans. on PAMI 13, 518–526 (2004)
16. Kreyszig, E.: Differential Geometry. Dover, New York (1991)
17. Evans, L.C., Gariepy, R.F.: Measure Theory and Fine Properties of Functions. CRC Press, Boca Raton (1992)
18. Kimmel, R., Bruckstein, A.M.: Regularized laplacian zero crossings and optimal edge integrators. In: Proc. of Image and Vision Computing (2001)
19. Leventon, M.E., Grimson, W.E.L., Faugeras, O.: shape influence in geodesic active contours. In: Proc. CVPR, pp. 316–323 (2000)
20. Rousson, M., Paragios, N.: Shape priors for level set representations. In: Proc. ECCV (2002)